Kinetic study of hydrogen sulfide absorption in aqueous chlorine solution

Jean-Baptiste Vilmain, Valérie Couroussé, Pierre-François Biard, Mohamed Azizi, Annabelle Couvert

Kinetic study of hydrogen sulfide absorption in aqueous chlorine solution

Jean-Baptiste VILMAIN[a,c], Valérie COUROUSSE[a,c], Pierre-François BIARD[a,b,c*], Mohamed AZIZI[a,c], Annabelle COUVERT[a,c]

[a]Ecole Nationale Supérieure de Chimie de Rennes, CNRS, UMR 6226, 11 Allée de Beaulieu, CS 50837, 35708 Rennes Cedex 7, France

[b]Université de Rennes 1, CNRS, UMR 6226, 3 rue du Clos-Courtel, BP 90433, 35704 Rennes Cedex 7, France

[c]Université européenne de Bretagne, 5 boulevard Laënnec, 35000 Rennes, France

Graphical abstract

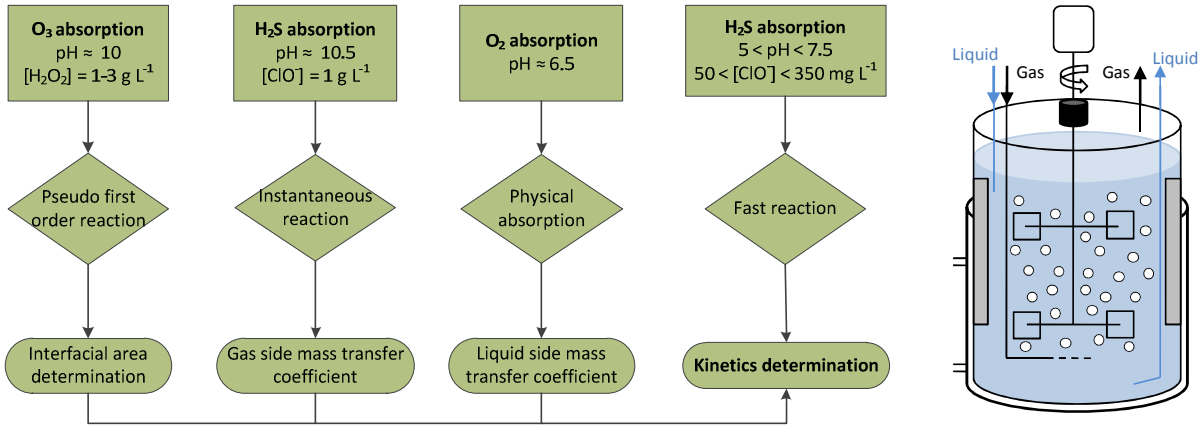

* Corresponding author: Pierre-François BIARD ; Tel: +33 2 23 23 81 57
Email-address: pierre-francois.biard@ensc-rennes.fr

Abstract

Hydrogen sulfide (H_2S) is currently removed from gaseous effluents by chemical scrubbing using water. Chlorine is a top-grade oxidant, reacting with H_2S with a fast kinetic rate and enhancing its mass transfer rate. To design, optimize and scale-up scrubbers, knowledge of the reaction kinetics and mechanism is requested. This study investigates the H_2S oxidation rate by reactive absorption in a mechanically agitated gas-liquid reactor. Mass transfer (gas and liquid sides mass transfer coefficients) and hydrodynamic (interfacial area) performances of the gas-liquid reactor were measured using appropriated physical or chemical absorption methods. The accuracy of these parameters was checked by modeling the H_2S absorption in water without oxidant. A sensitivity analysis confirmed the robustness of the model. Finally, reactive absorption of H_2S in chlorine solution for acidic or circumneutral pH allowed to investigate the kinetics of reaction. The overall oxidation mechanism could be described assuming that H_2S is oxidized irreversibly by both hypochlorite anion ClO^- ($k = 6.75\ 10^6$ L mol^{-1} s^{-1}) and hypochlorous acid ClOH ($k = 1.62\ 10^5$ L mol^{-1} s^{-1}).

Keywords

Hydrogen sulfide, chlorine, kinetics, mass transfer, absorption, scrubber

Highlights

- Kinetics of H_2S oxidation by chlorine is investigated using a well agitated reactor
- Mass transfer and hydrodynamics performances of the reactor are determined
- Sensitivity analysis is performed to assess the robustness of the modeling
- H_2S reacts irreversibly with hypochlorous acid and hypochlorite anion
- Kinetic constants are determined

1 Introduction

Hydrogen sulfide (H_2S) is a major toxic compound involved in odor emissions of many industries such as waste water treatment, pulp industry, etc. (Gostelow et al., 2001; Kangas et al., 1984; Rappert and Müller, 2005). Proving high and reliable efficiency, chemical wet scrubbing is the most widely used process to prevent H_2S emissions (Busca and Chiara, 2003; Smet and Langenhove, 1998; Smet et al., 1998). This technique involves H_2S mass transfer in an aqueous phase using a gas-liquid contactor. Since H_2S is poorly soluble in water, to increase its removal efficiency, aqueous oxidant solutions at basic pH are often used (Biard et al., 2009; Bonnin, 1991; Chen et al., 2001; Kerc and Olmez, 2010; Le Sauze et al., 1991). Other processes are currently used to remove H_2S : biofiltration, absorption in alkanolamine solutions, absorption using the Claus process or catalysts to recover the elemental sulfur, etc. (Busca and Chiara, 2003; Kohl and Nielsen, 1997).

Due to a strong reactivity with H_2S, chlorine is a top-grade oxidant for this application and is currently used, especially in waste water treatment plants, in rendering and composting facilities, etc. The process is operated semi-continuously (Biard et al., 2010). The scrubbing liquid is stored in a tank located at the bottom of the scrubber and is recirculated. pH and chlorine concentration are regulated. This scrubbing liquid is just drained when the salt accumulation due to H_2S oxidation into sulfate anions becomes too high.

Chlorine speciation in water is rather complex. Depending on the pH, the ionic strength and the chloride concentration, chlorine can be present in water mainly as aqueous chlorine Cl_2, hypochlorous acid ClOH and hypochlorite ions ClO^- (Deborde and Von Gunten, 2008):

$$Cl_2 + H_2O \rightleftarrows ClOH + H^+ + Cl^- \qquad \text{Eq. 1}$$

$$K_{Cl_2} = \frac{[ClOH][H^+][Cl^-]}{[Cl_2]} = 3.8\times10^{-4}\ mol^2\ L^{-2} \text{ at 293 K and a negligible ionic strength} \qquad \text{Eq. 2}$$

$$ClOH \rightleftarrows ClO^- + H^+ \qquad K_{A,1} = \frac{[ClO^-][H^+]}{[ClOH]} \text{ with } pK_{A,1} = 7.58 \text{ at 293 K} \qquad \text{Eq. 3}$$

Cl_2 exists only at acidic pH (pH < 5-6) and its coexistence domain increases with the total chloride concentration. Some additional species such as Cl_3^-, Cl_2O can be observed. However, at a low chloride concentration, they can be neglected (Deborde and Von Gunten, 2008). With a higher oxidation potential, ClOH currently reacts faster than ClO^-. These observations emphasize that oxidation kinetics with chlorine are pH dependant.

An excess of chlorine (at least 4 mol of chlorine for 1 mol of H_2S) can mineralize H_2S (oxidation number = -2) in sulfate ion (oxidation number = +6) according to the following global mechanism at alkaline pH:

$$H_2S + 4NaOCl + 2NaOH \xrightarrow{\text{complete oxidation}} Na_2SO_4 + 4NaCl + 2H_2O \quad \text{Eq. 4}$$

The first by-product formed after H_2S oxidation is elemental sulfur which can be further oxidized in sulfite SO_3^{2-} and sulfate SO_4^{2-} (Choppin and Faulkenberry, 1937). In the whole process, oxidation of elemental sulfur into sulfite is considered as the rate limiting step, especially at pH close to the neutrality where colloidal sulfur accumulation can be observed in chemical scrubbing processes (Biard et al., 2009; Bonnin, 1991).

H_2S is a weak diacid in equilibrium with its conjugated base, the hydrosulfide anion HS^- ($pK_{A,2}$ = 7.07 at 293°K (Roustan, 2003). The sulfide anion S^{2-} is present only at very basic pH and can be neglected ($pK_{A,3}$ = 13.94 at 293°K) at pH used in chemical scrubbing (pH ≤ 11-12). During H_2S chemical scrubbing in chlorine solutions, both H_2S dissociation in HS^- and oxidation decrease the H_2S bulk concentration, which maintains a maximal and constant mass transfer driving force. Moreover, since the kinetics of these reactions are really fast, mass transfer enhancement is currently observed, which leads to a large removal efficiency (Biard et al., 2010). Indeed, mass transfer enhancement due to these reactions enhances the absorption rate by decreasing the mass transfer resistance in the liquid film (Roustan, 2003). By this way, the whole resistance could be located in the gas phase. Mass transfer enhancement calculation is rather complicated and depends on several parameters: nature (reversible, irreversible) and number of reactions involved, reaction(s) kinetics, reaction(s) stoichiometry, concentrations and diffusion coefficients (van Swaaij and Versteeg, 1992).

Within the current operating conditions, which insure an excess of chlorine (several hundred mg L^{-1} are usually set), H_2S and HS^- cannot be measured in the liquid bulk since they are quickly oxidized in the liquid film at the vicinity of the gas-liquid interface. From wet scrubbing experiments in packed column, Bonnin (1991) determined an apparent kinetic constant between H_2S and ClOH of 1.8×10^8 L mol^{-1} s^{-1} for pH ranging from 9 to 11 at 293 K. However, this determination was based on wrong assumptions (Biard et al., 2010). Therefore, the kinetic rate of H_2S oxidation by chlorine is poorly known whereas it would enable better gas-liquid contactor scale-up, design and optimization.

To answer to this issue, the purpose of this study is to determine the H_2S oxidation kinetics at 293 K with ClOH and ClO^-. Only a few techniques like stopped flow or competitive methods or reactive absorption can be used to determine high kinetic constants (Beltrán, 2004). In this particular case, reactive absorption seems to be appropriated (Vaidya and Kenig, 2007b). This technique has been

successfully applied in the past to determine kinetic constants in the fields of ozonation, chlorine hydrolysis, flue desulfurization or CO_2 capture in amine solutions (Aieta and Roberts, 1986; Beltrán, 2004; Ebrahimi et al., 2003; Jia et al., 2010; Jing et al., 2012; Kucka et al., 2002; Sema et al., 2012; Sotelo et al., 1991; Vaidya and Kenig, 2007a, 2009).

During H_2S absorption, H_2S removal efficiency is governed by the mass transfer rate which depends on the hydrodynamic and mass transfer performances of the reactor, gas and liquid flow patterns and H_2S oxidation kinetic rate. If all these parameters are controlled, the kinetics can be investigated. To simplify the liquid flow pattern and to insure a homogeneous liquid phase, a gas-liquid contactor agitated by a Rushton turbine has been selected. First of all, the mass transfer and hydrodynamic parameters of the laboratory tank must be determined in controlled conditions (gas and liquid flow rates, pressure, rotation speed). These parameters are determined by physical absorption of oxygen and by chemical absorption of ozone and H_2S in specific mass transfer regimes. Then, the kinetic constant at 293 K can be deduced during H_2S absorption in chlorine solutions set at various concentrations and pH. Chlorine concentration must be optimized to find a compromise between a too low kinetic rate on the one hand and a too large kinetic rate on the other hand to enable an accurate enhancement factor determination. pH will be in the range 5-7.5 to assess the influence of the chlorine speciation and to limit the potential HS^- formation. The next section reviews the mass transfer theory which is required for the gas-liquid contactor characterization and the kinetic constant determination.

2 Mass transfer modeling

Gas-liquid mass transfer can be described according to various theories. Usually, the double film theory (explicative scheme in the supplementary material) is applied in steady state (Whitman, 1923). The molar flux transferred of any species A (dJ in mol m^{-2} s^{-1}) per square meter of gas-liquid area can be written (Perry and Green, 1997):

$$\mathrm{d}J = Ek_L\left(C_A^* - C_A\right) = K_L\left(C_A^{Eq} - C_A\right) \qquad \text{Eq. 5}$$

E is the so-called enhancement factor (no unit) which is the ratio of the absorption rate with and without the reaction for an identical difference $C_A^* - C_A$. Other definitions of the enhancement factor can be found in the literature. However, this one remains the most encountered. C_A, C_A^*, C_A^{Eq} are the solute concentration respectively in the bulk (mol m^{-3}), at the gas-liquid interface (superscript *) and in equilibrium (superscript Eq) with the gas phase concentration C_A^G deduced from the Henry's law:

$$C_A^{Eq} = \frac{p_A}{H_A} = \frac{R \times T \times C_A^G}{H_A} \qquad \text{Eq. 6}$$

p_A is the partial pressure (Pa), H_A the Henry's law constant (Pa m^3 mol^{-1}). k_L and K_L (Eq. 4) are respectively the local and overall liquid side mass transfer coefficients (m s^{-1}) which are linked together through the following relation:

$$\frac{1}{K_L} = \frac{1}{Ek_L} + \frac{RT}{H_A k_G} \qquad \text{Eq. 7}$$

k_G is the local gas side mass transfer coefficient. k_L and k_G order of magnitude are respectively 0.5-5 10^{-4} m s^{-1} and 0.5-5 10^{-2} m s^{-1} for most gas-liquid contactors (Roustan, 2003). The liquid-phase relative mass transfer resistance R_L , which represents the ratio of the resistance located in the liquid phase divided by the total resistance, is calculated by the following equation (Hoffmann et al., 2007; Rejl et al., 2009):

$$R_L = \left(1 + \frac{RTEk_L}{H_A k_G}\right)^{-1} \text{ and } R_G = 1 - R_L \qquad \text{Eq. 8}$$

In addition to the interface mass transfer and chemical kinetics, the performance of a gas-liquid contactor depends on the extent of mixing in both the phases (Joshi et al., 1982). Assuming that the liquid flow is perfectly mixed, *i.e.* complete back-mixing, the solute bulk concentration is uniform in the whole reactor which possesses an effective volume V (gas and liquid volumes sum). The extent of mixing for the gas phase depends on the impeller speed and the gas flow rate through the gas hold-

up (Lee and Pang Tsui, 1999). At a moderate impeller speed, the power input is not sufficient to disperse the gas in the part of the reactor located below the sparger. In this case, the extent of back-mixing is low and the flow can be considered as a plug flow. The role of the agitation is to break bubbles to maintain a high interfacial area. Assuming a plug flow for the gas and a perfectly mixed liquid, the absorption rate (N in mol s^{-1}) can be calculated by the following equation:

$$N = K_L a^{\circ} V \overline{\left(C_A^{Eq} - C_A\right)} = K_L a^{\circ} V \frac{\left(C_{A,i}^{Eq} - C_A\right) - \left(C_{A,o}^{Eq} - C_A\right)}{\ln \frac{C_{A,i}^{Eq} - C_A}{C_{A,o}^{Eq} - C_A}} \qquad \text{Eq. 9}$$

Subscripts i and o refer to the reactor inlet and outlet. $a°$ is the gas-liquid interfacial area (m^2 m^{-3}) relative to the effective volume V. The mass balance enables to write:

$$N = Q_G \left(C_{A,i}^G - C_{A,o}^G\right) \qquad \text{Eq. 10}$$

Q_G is the gas volume flow rates (m^3 s^{-1}). From Eqs. 6-10:

$$\ln \frac{\frac{RTC_{A,i}^G}{H_A} - C_A}{\frac{RTC_{A,o}^G}{H_A} - C_A} = K_L a^{\circ} \frac{VRT}{H_A Q_G} = \frac{a^{\circ}}{\frac{1}{Ek_L} + \frac{RT}{H_A k_G}} \frac{VRT}{H_A Q_G} \qquad \text{Eq. 11}$$

When the reaction rate is significantly larger than the mass transfer rate, the solute is entirely consumed in the liquid film and C_A tends toward 0. In the other cases, C_A depends on the liquid hold-up, liquid residence time and on the kinetic and mass transfer rates (Lee and Pang Tsui, 1999). Except for two limit cases (slow and instantaneous reactions in the liquid film), E depends on the reaction kinetics. Therefore, its determination in controlled and appropriated operating conditions could enable kinetics determination. k_L and k_G are mainly influenced by the properties and hydrodynamics of respectively the liquid and the gas phases. The interfacial area depends on the gas hold-up and bubbles size, which are determined by the flow field, the gas flow-rate, the power input and the gas dispersion characteristic of the impeller (RESI, 2013). Except the gas side mass transfer coefficient which has never been measured for a gas-liquid agitated tank, they can be estimated using semi-empirical correlations (Calderbank, 1958; Calderbank, 1959; Joshi et al., 1982; Lee and Pang Tsui, 1999). In this study, for a better accuracy, they will be determined prior to E measurements.

3 Material and methods

Different chemical systems were implemented to determine $a°$ (ozone absorption in a solution of hydrogen peroxide), k_L (physical absorption of pure oxygen), k_G (chemical absorption of H_2S in highly concentrated chlorine alkaline solution) and E (H_2S chemical absorption in slightly acidic or neutral chlorine solution) (Table 1). H_2S absorption in pure water was also investigated to assess the accuracy of $a°$, k_L and k_G determination. The parameters are deduced from the removal efficiency (Eq. 12) of each absorbed species:

$$Eff_A = \frac{C_{A,i}^G - C_{A,o}^G}{C_{A,i}^G} \qquad \text{Eq. 12}$$

Table 1: Synthesis of the physical and chemical operating conditions applied.

	Parameter	Value	Experimental uncertainty
Physical operating conditions			
	Temperature T	293 K	± 1 K
	Effective volume V	1.65 L	± 0.05 L (3%)
	Impeller speed	250 rpm	
	Liquid flow rate Q_L	7-30 L h^{-1}	3.0%
	Gas flow rate Q_G	400-750 NL h^{-1}	3.1%
Chemical operating conditions			
$a°$ measurement O_3 absorption in H_2O_2 solution	Inlet H_2O_2 concentration	1173-2720 mg L^{-1}	2.1%
	pH	9.9-10.15	± 0.1 unit
	Inlet O_3 concentration	35-60 g Nm^{-3}	2%
k_L measurement O_2 physical absorption	pH	6.5	± 0.1 unit
	Inlet O_2 concentration	Pure oxygen	
k_G measurement H_2S absorption in ClOH solution	pH	10.4-10.8	± 0.1 unit
	Inlet H_2S concentration	110-135 mg Nm^{-3}	10%
	Inlet chlorine concentration	1 g.L^{-1}	2.1%
Absorption of H_2S in water	pH	8-8.1	± 0.1 unit
	Inlet H_2S concentration	50-65 mg Nm^{-3}	10%
Absorption of H_2S in chlorine solution	pH	5-7.5	± 0.1 unit
	Inlet H_2S concentration	50-150 mg Nm^{-3}	10%
	Inlet chlorine concentration	50-350 mg L^{-1}	2.1%

3.1 Presentation of the experimental set-up

The laboratory-scale glass gas-liquid contactor (*1* in Fig. 1) is a nominal 2 liters tank mechanically agitated by a Rushton turbine (impeller diameter of 4.5 cm and vessel diameter of 11.0 cm). The liquid phase is prepared in a 50 L Nalgene® storage tank (*2*) using demineralized water. Concentrated NaOH or H_3PO_4 solutions are added to set the pH. Depending on the chemical system implemented, chlorine or hydrogen peroxide can be also added to set a given oxidant concentration. The reactor is fed and drained by an inlet (*3*) and an outlet centrifugal pumps (*4*). Flow rates are controlled by means of valves and measured by two flowmeters (*3',4'*). The contactor temperature is controlled at 20 ± 1 °C with an isothermal liquid circulating in the reactor jacket (*5*). The pH of the liquid and the temperature are measured on-line using a combined pH-probe (*6*). Fresh air is introduced using a gas pump (*7*). Then a gas flow of N_2-H_2S (*8*) is mixed with the pumped air thanks to a static mixer (*10*). These two flows are controlled by means of valves and measured by float-type flowmeters (*7',8'*) (Sho Rate R6-15-C and R6-15-D) and dispersed in the reactor by a titanium sparger (*11*). Before starting the experiments, the gas-liquid contactor is by-passed to analyze the gas inlet at steady-state. For the interfacial area determination, the feed system is replaced by an ozone generator fed with oxygen. In this case, the ozone flow rate is controlled by a flowmeter in Teflon®. During the experiments, a fraction of the gas is by-passed to analyze the outlet at steady-state (*12*). Before being released in the atmosphere, residual O_3 and H_2S in the gas phase were quenched using respectively an ozone destructor and by bubbling in a concentrated basic chlorine solution (*13*). The gas pressure is measured twice, at the flowmeter outlet to correct the flow rate and in the reactor headspace, using manometers.

Each float-type flowmeter has been calibrated under controlled pressure and temperature. The read gas flow-rate must be corrected taking into account pressure and temperature variability using the following relations (Perry and Green, 1997):

$$Q_G\left(\text{NL.h}^{-1}\right) = Q_{G,read}\left(\text{NL.h}^{-1}\right)\sqrt{\frac{PT_{calib.}M_{calib.}}{P_{calib.}TM}} \text{ and } Q_G\left(\text{L.h}^{-1}\right) = Q_{G,read}\left(\text{L.h}^{-1}\right)\sqrt{\frac{TP_{calib.}M_{calib.}}{T_{calib.}PM}} \qquad \textbf{Eq. 13}$$

The subscripts "calib" refers to the conditions used during the calibration. Values of the physico-chemical properties and a list of the suppliers and references of the chemical compounds and equipments used are respectively presented in Tables A.1 and A.2.

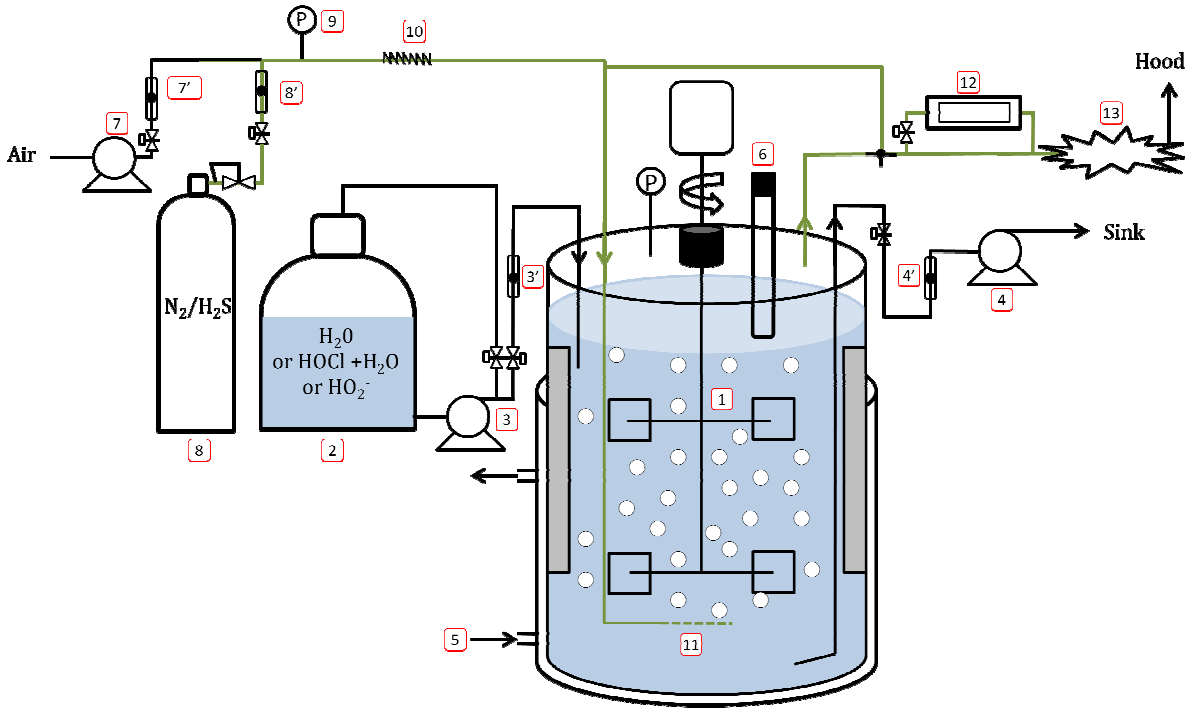

Figure 1: Scheme of the experimental set-up.

3.2 Analysis

Chlorine and hydrogen peroxide were analyzed by the iodometric method. An excess of iodide potassium was oxidized in diode at acidic pH (use of HCl for H_2O_2 and of CH_3COOH for ClOH) which was titrated by sodium thiosulfate. Ammonium heptamolybdate at 5 g L^{-1} was added for H_2O_2 analysis to catalyze the I_2 formation.

H_2S in the gas phase was bubbled continuously at a controlled flow rate of 50 L h^{-1} (at ambient temperature and pressure) in a 90 mL concentrated chlorine solution (500 mg L^{-1}) at pH = 9, and then, oxidized into sulfate ions. Then the sulfates formed were analyzed by ion chromatography with conductivity detection. The H_2S concentration was deduced from the amount of sulfate anion and the volume of gas trapped.

O_3 was analyzed in the gas phase using an UV ozone analyzer. Measurements of dissolved O_3 and H_2S were not necessary since they were rapidly oxidized in the chemical system implemented and therefore could not be detected. For k_G determination, a membrane covered galvanic sensor was used to measure dissolved oxygen concentration.

4 Results and discussion

4.1 Hydrodynamics of the gas-liquid contactor

The assumption of the complete liquid back mixing (perfectly mixed liquid phase) has been checked by Residence Time Distribution (RTD) experiments for various gas (0 to 800 NL h^{-1}) and liquid (20 to 80 L h^{-1}) flow rates and impeller speed (100 to 800 rpm) using fluorescein as a tracer. It showed that the liquid was perfectly mixed while the impeller speed is larger than 100 rpm whatever the flow rate in the range implemented.

The gas flow pattern cannot be determined by RTD measurement due to a too low residence time (few seconds) which is not compatible with usual sensor time response. However, we can assume that the gas back mixing is almost negligible since the impeller speed is lower than the minimal speed necessary to disperse the gas below the sparger. Indeed, according to the relations cited by Lee and Pang Tsui (1999), a minimal speed of 800-1000 rpm is expected for the gas flow rate range tested. This was confirmed by visual observation. Since the gas loading was rather low, the elevation of the liquid level after starting the gas dispersion was not significant confirming a gas hold-up lower than 1.5%.

The interfacial area $a°$ can be determined in the pseudo first-order chemical absorption regime (Hoffmann et al., 2007; Rejl et al., 2009). Chemical absorption of ozone in an aqueous solution doped with hydroperoxyde anions HO_2^- can be satisfactorily used, especially considering that ozone is poorly soluble in water (H_A is large) which allows to neglect the gas phase resistance ($R_G \rightarrow 0$ and $k_L \approx K_L$). HO_2^-, the conjugated base of H_2O_2, initiates the O_3 decomposition according to the following bimolecular irreversible reaction (Staehelin and Hoigne, 1982):

$$O_3 + HO_2^- \xrightarrow{k_{O_3/HO_2^-} = 2.8\,10^9\ m^3\ mol^{-1}\ s^{-1}} O_3^- + HO_2° \qquad \text{Eq. 14}$$

If H_2O_2 is introduced in large amount and at a basic pH, the ozone consumption is fast in the liquid film which means that O_3 does not reach the liquid bulk. Consequently, O_3 is entirely consumed by HO_2^- and not by any parasite compound or radical formed after its decomposition with the net consumption of one mol of H_2O_2 for one mol of O_3 transferred (Biard, 2009). Therefore, according to Eq. 11:

$$\ln\frac{C^G_{O_3,i}}{C^G_{O_3,o}} = Ek_L a° \frac{VRT}{H_{O_3} Q_G} \qquad \text{Eq. 15}$$

Moreover, since the H_2O_2 deprotonation into HO_2^- is really faster than ozone consumption by HO_2^- and since $C_{H_2O_2} >> C^*_{O_3}$, the HO_2^- concentration remains constant in the diffusional film (pseudo first-order absorption regime). In this case (Hikita and Asai, 1964):

$$E = \frac{Ha}{\tanh(Ha)} \qquad \text{Eq. 16}$$

Ha (Hatta number) is a dimensionless number:

$$Ha = \sqrt{\frac{k_{O_3/HO_2^-} C_{HO_2^-} D_{O_3}}{k_L^{\,2}}} \qquad \text{Eq. 17}$$

D_i is the liquid diffusion coefficient of any species i. If the reaction kinetics is fast in the liquid film (Ha >3), tanh(*Ha*) tends towards 1. Therefore:

$$\ln\frac{C^G_{A,i}}{C^G_{A,o}} = Hak_L a^\circ \frac{VRT}{H_{O_3} Q_G} = \sqrt{k_{O_3/HO_2^-}[HO_2^-]D_{O_3,L}}\, a^\circ \frac{VRT}{H_{O_3} Q_G} \qquad \text{Eq. 18}$$

Consequently:

$$a^\circ = \frac{-\ln\left(1 - Eff_{O_3}\right)}{\sqrt{k_{O_3/HO_2^-}[HO_2^-]D_{O_3}}} \frac{Q_G H_{O_3}}{VRT} \qquad \text{Eq. 19}$$

In a given gas-liquid mechanically agitated vessel, *a*° depends on the gas flow rate, impeller speed and liquid properties (ionic strength, presence of surfactant). Consequently, these parameters must be controlled. Since *a*° does not depends on the absorbed species, extrapolation from O_3 to H_2S chemical system is not an issue. However, the ionic strength must be kept low to have identical properties between both chemical systems. *a*° has been determined for various gas flow rates and H_2O_2 concentrations at *pH* = 10. The HO_2^- concentration in the contactor was deduced from the pH measured and the H_2O_2 concentrations at the inlet, and the mass balance considering that one mol of O_3 transferred consumed one mol of H_2O_2.

In the thin range of studied superficial velocity, *a*° is not statistically dependent on the velocity (Table A.3 in appendix). An average value of 76.1 ± 4.9 $m^2\ m^{-3}$ is found (Relative Standard Deviation RSD = 6%). The average value of *a*° is in agreement with the order of magnitude expected. The standard deviation stays within the calculated 10% experimental uncertainty. The parity plot (Fig. 2) confirms a good agreement between the experimental and theoretical (using Eq. 19 and *a*° = 76.1 $m^2\ m^{-3}$) Eff_{O_3} values. The values of the Hatta number, using the k_L value measured later (§ 4.2), are larger than 3, confirming the fast reaction assumption (Table A.3 in appendix).

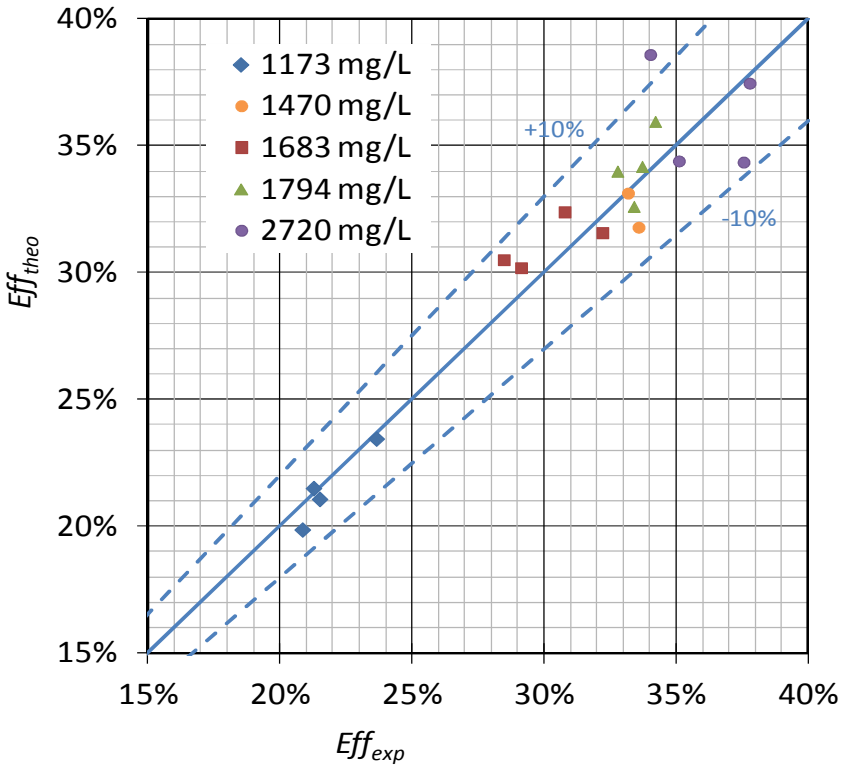

Figure 2: Parity diagram comparing the experimental values of the ozone removal efficiency with the theoretical values obtained with $a° = 76.1\ m^2\ m^{-3}$ for various H_2O_2 concentrations.

4.2 Liquid-side mass transfer coefficient determination

The liquid side mass transfer coefficient k_L depends on the absorbed species diffusion coefficient, the liquid properties (viscosity, density) and the liquid hydrodynamics. k_L can be determined by chemical or physical methods (Hoffmann et al., 2007; Rejl et al., 2009). Chemical methods results can be biased by the reactant added which can affect the liquid properties. The only restriction linked to the physical absorption method is the requirement of a poorly soluble compound to avoid reaching the gas-liquid equilibrium and limit the gas-phase resistance ($R_G \rightarrow 0$) (Lara Marquez et al., 1994). Consequently, the physical absorption of pure oxygen at steady-state has been selected. In this case:

$$C_{O_2,i}^{Eq} = C_{O_2,o}^{Eq} = \frac{p_{O_2}}{H_{O_2}} \qquad \text{Eq. 20}$$

Therefore, since the liquid phase is perfectly mixed, the driving force is constant in the whole volume of the gas-liquid contactor:

$$\overline{\left(C_{O_2}^{Eq} - C_{O_2}\right)} = \frac{p_{O_2}}{H_{O_2}} - C_{O_2,o} \qquad \text{Eq. 21}$$

The mass transfer equation (Eq. 8) coupled with the mass balance equation leads to Eq. 22:

$$N = k_L a^{\circ} V \left(\frac{p_{O_2}}{H_{O_2}} - C_{O_2,o} \right) = Q_L \left(C_{O_2,o} - C_{O_2,i} \right) \qquad \text{Eq. 22}$$

$$\Rightarrow k_L = \frac{Q_L \left(C_{O_2,o} - C_{O_2,i} \right)}{a^{\circ} V \left(\frac{p_{O_2}}{H_{O_2}} - C_{O_2,o} \right)} \qquad \text{Eq. 23}$$

Q_L is the liquid volume flow rate ($m^3\ s^{-1}$). $\frac{p_A}{H_{O_2}}$ corresponds to the O_2 concentration at saturation in the liquid which can be measured in the semi-continuous mode waiting for the saturation. No significant effect of the gas and liquid flow rates on k_L has been emphasized (Table 2). An average value of $k_L^{O_2}$ = $2.7\times10^{-4} \pm 0.25\times10^{-4}$ m s^{-1} (RSD = 9%) was found which is totally in agreement with the expected value. The H_2S liquid side mass transfer coefficient must be extrapolated from the oxygen one by the following relation (Roustan, 2003):

$$\frac{k_L^{H_2S}}{k_L^{O_2}} = \sqrt{\frac{D_{H_2S}}{D_{O_2}}} \Rightarrow k_L^{H_2S} = 2.5\times10^{-4} \pm 0.2\times10^{-4}\ \text{m s}^{-1} \qquad \text{Eq. 24}$$

Table 2: Results of the oxygen absorption experiments.

Q_G (NL h^{-1})	426	426	469	469	469	509	509	509
U_{SG} (cm s^{-1})	1.24	1.24	1.37	1.37	1.37	1.49	1.49	1.49
Q_L (L h^{-1})	21.2	28.6	13.9	21.2	28.6	13.9	21.2	28.6
$10^4 \times k_L$ (m s^{-1})	2.29	2.55	2.43	2.89	2.80	2.89	2.79	2.98

4.3 Gas-side mass transfer coefficient determination

To measure the gas side coefficient, the liquid resistance must be negligible ($R_L \rightarrow 0$) which is the case when E is very large due to a very fast chemical reaction with a large excess of the reagents. Moreover, the solute is instantaneously consumed at the gas-liquid interface (C_A = 0). According to Eq. 11 :

$$\ln \frac{C_{A,i}^G}{C_{A,o}^G} = \frac{k_G a^{\circ} V}{Q_G} \Rightarrow k_G = -\frac{Q_G}{a^{\circ} V} \ln(1 - Eff) \qquad \text{Eq. 25}$$

k_G has been measured by H_2S absorption in an alkaline chlorine solution (10.5 < pH < 11 and C_{ClOH} = 1 g L^{-1}) for various gas and liquid flow rates (500 < Q_G < 550 NL h^{-1}). No significant effect of the flow rates on k_G has been emphasized. An average value of k_G = $4.2\times10^{-3} \pm 0.33\times10^{-3}$ m s^{-1} (RSD = 8%) was found.

The k_G value is a rather low and comparable to the values found in packed or spraying columns. Since it has never been measured for a mechanically agitated vessel, there is no possibility to discuss the validity of this result. In the case of H_2S, which is rather poorly soluble in water, the mass transfer resistance in the gas side (R_G) must not be neglected, especially with increasing E values in the liquid phase (Fig. 3). This result is very important for the following step. Indeed, the enhancement factor obtained during the H_2S absorption in chlorine solution should not be too large to limit as much as possible the gas-side resistance and improve the sensitivity of the calculations.

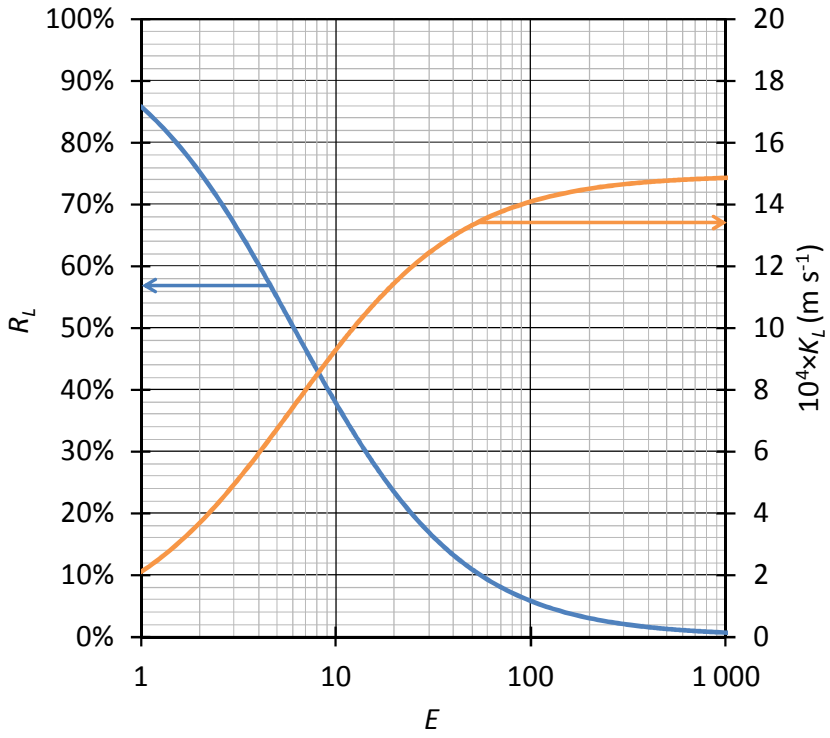

Figure 3: Liquid-phase relative mass transfer resistance R_L and overall liquid-phase mass transfer coefficient K_L vs. the enhancement factor E.

4.4 Validation of the mass transfer and hydrodynamic parameters

4.4.1 H_2S absorption in slightly alkaline water

The accuracy of $a°$, k_L and k_G values has been evaluated for H_2S absorption in water at alkaline pH (NaOH was added) using the operating conditions synthesized in Table 1. The pH was slightly alkaline to improve the H_2S removal efficiency (>20%) at a level sufficient to limit the experimental uncertainty.

Without H_2S oxidation and assuming that S^{2-} is negligible at the working pH, C_A can be deduced from the mass balance equation:

$$N = Q_G\left(C^G_{H_2S,i} - C^G_{H_2S,o}\right) = Q_L C_{H_2S}\left(1+10^{pH-pK_{A,2}}\right) \quad \text{Eq. 26}$$

According to Eqs 11 and 26:

$$\ln\left(\frac{A\left(1+10^{pH-pK_{A,2}}\right)-Eff_{H_2S}}{A\left(1+10^{pH-pK_{A,2}}\right)\left(1-Eff_{H_2S}\right)-Eff_{H_2S}}\right) = K_L a^\circ \frac{AV}{Q_L} \quad \text{Eq. 27}$$

A is the absorption rate (no unit) defined by Eq 28:

$$A = \frac{Q_L RT}{Q_G H_{H_2S}} \quad \text{Eq. 28}$$

This equation provides a limit value of Eff_{H_2S} since the term in the logarithm must be positive:

$$Eff_{\max} = \frac{A\left(1+10^{pH-pK_{A,2}}\right)}{1+A\left(1+10^{pH-pK_{A,2}}\right)} \quad \text{Eq. 29}$$

$Eff_{\max}$ is obtained when the chemical equilibrium is reached between the gas at the outlet and the liquid. It is the maximal removal efficiency for given pH, temperature and gas and liquid flow rates. Finally, from Eq. 29:

$$Eff_{H_2S} = \frac{A\left(1+10^{pH-pK_{A,2}}\right)\left(1-\exp\left(K_L a^\circ \frac{AV}{Q_L}\right)\right)}{1-\left(A\left(1+10^{pH-pK_{A,2}}\right)+1\right)\exp\left(K_L a^\circ \frac{AV}{Q_L}\right)} \quad \text{Eq. 30}$$

H_2S mass transfer in water can be enhanced thanks to the H_2S dissociation (E_{diss}) and/or recombination with HO^- (E_{HO^-}) which form HS^- in the liquid film (Biard and Couvert, 2013). This phenomenon is highly influenced by the pH. Assuming that these reactions are instantaneous comparing to mass transfer, the enhancement factors for each reaction can be calculated for each experimental point (Biard and Couvert, 2013). The global enhancement factor can be calculated for 2 instantaneous reactions by the sum of the individual enhancement factor minus 1 (Chang and Rochelle, 1982; van Swaaij and Versteeg, 1992). Then, it leads to:

$$\begin{aligned} E_\infty &= E_{HO^-} + E_{\text{diss}} - 1 \\ E_{HO^-} &= 1 + \frac{D_{HO^-}\,10^{pH-pK_w}}{\frac{D_{H_2S}D_{HO^-}}{D_{HS^-}\times 10^{pK_w - pK_{A,2}}} + D_{H_2S}C^*_{H_2S}} \\ E_{\text{diss}} &= 1 + \frac{\sqrt{\left(D_{H^+}10^{-pH} + D_{HS^-}C_{HS^-}\right)^2 - 4\left(1-C^*_{H_2S}/C_{H_2S}\right)\left(D_{H^+}10^{-pH}D_{HS^-}C_{HS^-}\right)} - \left(D_{H^+}10^{-pH} + D_{HS^-}C_{HS^-}\right)}{2D_{H_2S}\left(C^*_{H_2S} - C_{H_2S}\right)} \end{aligned} \quad \text{Eq. 31}$$

pk_W is the negative log of the water ion product. The dissociation enhancement factor is low and included in the range 1.01-1.05 while the recombination with HO^- enhancement factor is in the range 1.18-1.29.

Comparison between the experimental removal efficiency and the theoretical values deduced from Eqs 30 and 31 is really good (Fig. 4). For low values of A, the equilibrium is almost reached since the removal efficiency is rather close of the maximal removal efficiency obtained from Eq. 29.

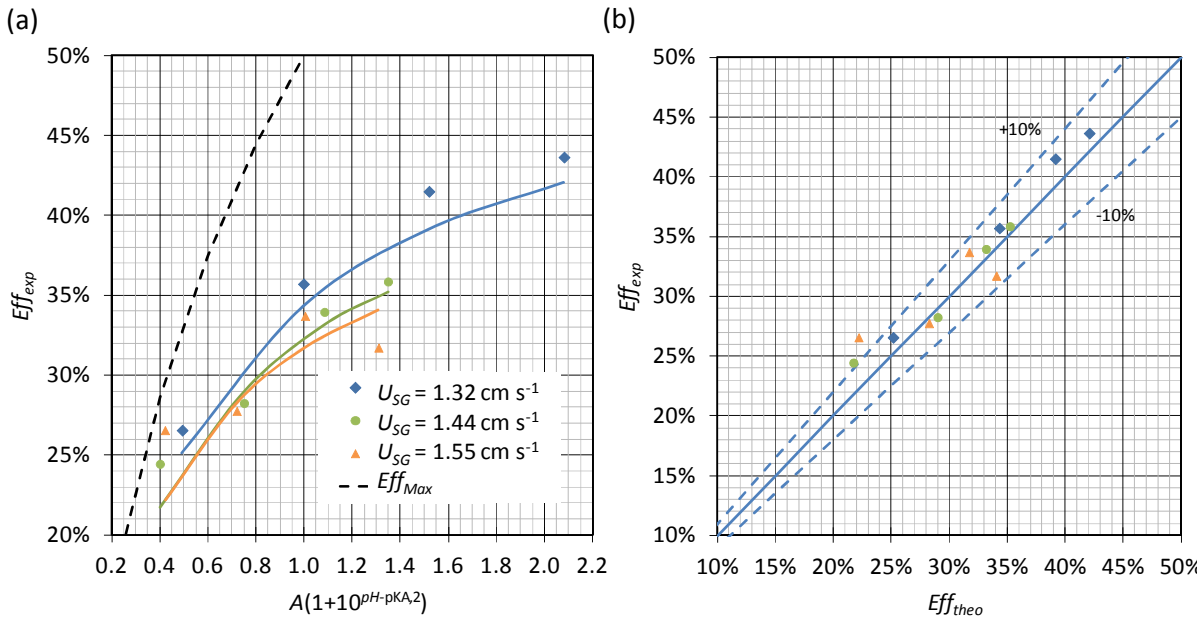

Figure 4: (a). H_2S removal efficiency vs. $A(1+10^{pH-pK_{A,2}})$ for various gas flow rates without chlorine. The colored lines represent the prediction of the model (Eq. 30) and the black line represents the prediction of the maximal removal efficiency (Eq. 29). (b). Parity plot between the experimental and predicted removal efficiencies.

4.4.2 Sensitivity analysis

The good agreement between the experimental and the theoretical values is not a sufficient condition to confirm the accuracy of the mass transfer coefficients and interfacial area determined previously and the robustness of the model. Indeed, each parameter has a variable influence on the removal efficiency. This influence can be assessed through a sensitivity analysis based on the elasticity index determination. The sensitivity analysis quantifies the effect of possible change in inputs on the model output which is here the removal efficiency (Asadi Kalameh et al., 2012; Yin et al., 2005). Consequently, it addresses the relative significance of potential errors in various input parameters. The elasticity index $EI_{P/Eff}$ measures the relative change of the removal efficiency for a relative change in an input parameter P. For example, for the input k_L :

$$EI_{k_L/Eff} = \frac{k_L}{Eff_{\text{for } k_L}} \times \frac{1}{2}\left[\frac{Eff_{\text{for } k_L + \Delta k_L} - Eff_{\text{for } k_L}}{\Delta k_L} + \frac{Eff_{\text{for } k_L - \Delta k_L} - Eff_{\text{for } k_L}}{-\Delta k_L}\right] \quad \text{Eq. 32}$$

Eff_{H_2S} must be a monotonic function of the input parameter P. The average elasticity indexes, taking into account all the experimental points, have been estimated for all the input of Eq. 30 for a relative change of 10% (Table 3). The indexes for the input Q_G and H_{H_2S} are negative since *Eff* is a decreasing function of *them*. Except for the *pH*, the standard deviation is low, demonstrating that EI is almost constant. Results of Table 3 emphasize that *Eff* is mainly sensitive to two measured variables, *pH* and Q_G, and two physico-chemical constants, $pK_{A,2}$ and $H_{H_2S,}$ whose the values taken from the literature are consistent between many authors and should be precise. Consequently, the difference between the experimental and the theoretical values of Eff_{H_2S} (Fig. 4) might be mainly due to the experimental errors of the *pH*, and in a lower extent of Q_G, more than uncertainties of k_L, k_G and $a°$ determined previously. On the one hand, *pH* was rather unsteady and affected by the gas bubbles with a low precision of ± 0.1 unit. On the other hand, Q_G was measured with a limited combined uncertainty of 3.1% taking into account the uncertainties of the variable area flowmeter, the pressure and the temperature measurements used for the flow rate correction. The strong sensitivity of *Eff* to the *pH* and $pk_{A,2}$ can be explained by the fact that these inputs affect significantly the difference of H_2S concentrations between the interface and the bulk (mass transfer driving force).

Table 3: Elasticity index determination for Eff_{H_2S} and $K_La°$.

Removal efficiency (Eff_{H_2S})								
Input parameter	*pH*	$pK_{A,2}$	Q_G	H_{H_2S}	$a°$ and V	E and k_L	Q_L	k_G
Average EI	4.83	2.30	-0.81	-0.73	0.45	0.37	0.36	0.079
Standard deviation	1.42	0.93	0.04	0.05	0.07	0.06	0.11	0.013
Overall liquid mass transfer coefficient ($K_La°$)								
Input parameter						E and k_L		k_G
Average EI						0.83		0.17
Standard deviation						0.004		0.004

The removal efficiency (Eff_{H_2S}) is also significantly influenced by $a°$ and V (which possesses a low experimental uncertainty of 3.0%), proving the $a°$ value determined previously is coherent and confirming the order of magnitude. The EI determination for E and k_L shows that Eff_{H_2S} is moderately sensitive to these parameters. Consequently, the order of magnitude of E and k_L should be coherent. On the contrary, Eff_{H_2S} is almost independent of k_G since the gas phase resistance is low (15% for E close to 1 according to Fig. 3). This is confirmed by the sensitivity index calculation of $K_La°$ for the input k_G (EI_{k_La/k_G}) which is 5 times lower than EI_{k_La/k_L} and $EI_{k_La/E}$ (Table 3). By the way, the k_G value found previously cannot be validated. To limit the influence of this uncertainty on the E determination using chlorine, the gas-phase resistance should be kept low as demonstrated by Fig. 3.

Moreover, Fig. 3 highlights an asymptotic behavior which emphasizes that $K_La°$ becomes less sensitive to *E* when *E* increases which could affect the uncertainty of the kinetic study.

4.5 Oxidation kinetics investigation

4.5.1 Enhancement factor determination

Table 4: Results of the H_2S reactive absorption in chlorine solutions.

pH	C_{NaOCl} (ppm)	$C^G_{H_2S}$ (10^3 mol m^{-3})	y† (%)	E_{exp}	E_{theo}	E_{39}/E_{39+40}‡ (%)	Eff_{exp} (%)	Eff_{theo} (%)	Error (%)
4.90	293	1.50	84.3	7.0	5.41	38.5	89.0	85.6	4.0
4.92	301	1.65	83.2	6.4	5.49	38.8	88.0	86.1	2.3
4.93	305	1.43	85.3	7.5	5.55	39.5	89.7	86.0	4.3
4.94	222	2.50	73.9	3.6	4.69	38.6	79.3	84.3	5.9
4.95	229	2.38	75.2	3.8	4.78	39.1	80.4	84.4	4.8
4.95	233	2.01	78.5	4.8	4.83	39.7	83.6	83.8	0.2
5.59	278	1.19	88.6	4.2	6.64	67.4	79.4	86.8	8.5
5.59	282	1.25	88.1	3.9	6.66	67.0	78.1	86.8	10.0
5.58	284	1.28	87.9	3.8	6.66	66.7	77.8	86.9	10.5
5.80	45	2.17	70.0	2.3	2.86	74.8	68.7	74.4	7.8
5.88	170	2.05	80.6	5.2	6.01	76.9	85.1	87.2	2.4
5.88	178	2.12	80.4	5.0	6.15	76.8	84.3	87.5	3.5
5.88	182	2.07	80.9	5.2	6.23	76.9	85.2	87.8	3.0
5.99	351	1.78	87.8	9.6	9.64	82.1	90.0	90.1	0.0
5.99	365	1.72	88.3	10.0	9.85	82.2	90.3	90.2	0.1
6.04	202	1.21	90.1	9.6	7.76	84.5	92.0	90.1	2.1
6.50	187	1.47	91.2	6.9	11.25	93.8	88.7	93.1	4.7
6.51	191	1.45	91.5	7.0	11.48	94.0	88.9	93.2	4.6
6.94	269	0.39	98.6	27.8	21.13	97.9	96.6	95.9	0.7
7.53	257	0.46	98.9	23.6	32.10	99.4	96.2	96.8	0.7
7.53	265	0.25	99.4	44.1	32.67	99.4	97.3	96.8	0.4

Chemical absorption of H_2S was realized at various chlorine concentration and *pH* (Table 4). Since the H_2S oxidation rate is higher than the H_2S mass transfer rate and the Damkölher number is large (10 to 30), C_A can be neglected comparing to C^{Eq}_A (Roustan). In this case, according to Eq. 11, $K_La°$ and E_{exp} can be deduced for each experiment by respectively Eqs 33 and 7:

$$\ln\frac{C^G_{H_2S,i}}{C^G_{H_2S,o}} = K_La^\circ\frac{VRT}{H_{H_2S}Q_G} \Rightarrow K_La^\circ = -\frac{H_{H_2S}Q_G}{VRT}\ln\left(1-Eff_{H_2S}\right) \qquad \text{Eq. 33}$$

† x was comprised between 0.98 and 1.00 demonstrating that the reaction with ClOH is pseudo-first order.
‡ Represents the ratio of E obtained considering only the reaction 39 on E considering both reactions 39 and 40.

The results show that E_{exp} (i.e. the oxidation kinetic rate) increases obviously with the chlorine concentration but also surprisingly with the pH. Indeed, ClOH is considered as more reactive than ClO^- which lets expect a larger kinetic rate for lower pH. It might emphasize that HS^- plays a role in the oxidation mechanism, even if at the implemented pH, the HS^- concentration is significantly lower than the H_2S concentration. We note that E_{exp} values were included in the range 2.3-44, confirming that H_2S is entirely consumed in the liquid film for most experiments.

4.5.2 Kinetic constants determination

According to the experimental results, the oxidation mechanism might involve both acid-base and oxidation reactions. Indeed, H_2S and HS^- can be both oxidized by ClO^- or ClOH. A list of the potential reactions is presented in Table 5.

According to Eigen (1964), k_1 and k_3 values should be close to 3×10^{10} and 10^9 L mol^{-1} s^{-1}. The increasing of the kinetic rate with the pH can be due to the fact that a part of H_2S reacts with ClO^- in the liquid film to form HS^- (reaction 36) which can be further oxidized by ClOH (oxidation with ClO^- is unexpected according to the order of magnitude of k_4 and k_5). Moreover, ClOH can oxidize directly H_2S. If we assume that reverse reaction 36 is negligible, then the whole mechanism can be reduced to the two irreversible reactions 39 (equivalent to reaction 36 followed by reaction 37) and 40; and the two kinetic constants k_6 and k_7 must be determined.

Table 5 : H_2S oxidation mechanism. k_{-2} value and k_1 and k_3 orders of magnitude were obtained from (Eigen, 1964). k_4 and k_5 orders of magnitude were obtained from (Deborde and von Gunten, 2008).

Reaction		Type	Equilibrium constant
$H_2S + HO^- \underset{k_{-1}\approx 2.4\ 10^3\ s^{-1}}{\overset{k_1\approx 3\ 10^{10}\ L\ mol^{-1}\ s^{-1}}{\rightleftharpoons}} HS^- + H_2O$	Eq. 34	Acid-base	$K=\frac{k_1}{k_{-1}}=10^{-pK_{A,2}+pK_w}$
$H_2S + H_2O \underset{k_{-2}=7.5\ 10^{10}\ L\ mol^{-1}\ s^{-1}}{\overset{k_2=6.24\ 10^3\ s^{-1}}{\rightleftharpoons}} HS^- + H^+ + H_2O$	Eq. 35	Acid-base	$K=\frac{k_2}{k_{-2}}=10^{-pK_{A,2}}$
$H_2S + ClO^- \underset{k_{-3}\approx 3\ 10^8\ L\ mol^{-1}\ s^{-1}}{\overset{k_3\approx\ 10^9\ L\ mol^{-1}\ s^{-1}}{\rightleftharpoons}} HS^- + ClOH$	Eq. 36	Acid-base	$K=\frac{k_3}{k_{-3}}=10^{pK_{A,1}\ -\ pK_{A,2}}$
$HS^- + ClOH \xrightarrow{k_4\approx 5\ 10^8\ L\ mol^{-1}\ s^{-1}} S + Cl^- + H_2O$	Eq. 37	HS^- oxidation	
$HS^- + ClO^- \xrightarrow{k_5\approx 10^4\ L\ mol^{-1}\ s^{-1}} S + Cl^- + HO^-$	Eq. 38	HS^- oxidation	
$H_2S + ClO^- \xrightarrow{k_6} S + Cl^- + H_2O$	Eq. 39	H_2S oxidation	
$H_2S + ClOH \xrightarrow{k_7} S + HCl + H_2O$	Eq. 40	H_2S oxidation	

The enhancement factor for two irreversible parallel reactions in the liquid film can be determined using the Onda and coworkers approximated solution for the two-film theory (Biard et al., 2010; Onda et al., 1970). From the material balances and the boundary conditions:

$$E = \frac{1 - \frac{C_{H_2S}}{C^*_{H_2S}} + \frac{C_{ClOH}}{C^*_{H_2S}}\left[\frac{D_{ClOH}}{D_{H_2S}}\left(1 - \frac{C^*_{ClOH}}{C_{ClOH}}\right) + \frac{D_{ClO^-}}{D_{H_2S}}\left(\frac{C_{ClO^-}}{C_{ClOH}} - \frac{C^*_{ClO^-}}{C_{ClOH}}\right)\right]}{1 - C_{H_2S}/C^*_{H_2S}} \qquad \text{Eq. 41}$$

Due to the fast oxidation of H_2S in solution, the bulk concentration is negligible compared to the interface concentration:

$$E = 1 + \frac{C_{ClOH}}{C^*_{H_2S}}\left[\frac{D_{ClOH}}{D_{H_2S}}\left(1 - \frac{C^*_{ClOH}}{C_{ClOH}}\right) + \frac{D_{ClO^-}}{D_{H_2S}}\left(\frac{C_{ClO^-}}{C_{ClOH}} - \frac{C^*_{ClO^-}}{C_{ClOH}}\right)\right]$$

$$\Rightarrow E = 1 + \frac{D_{ClOH}}{D_{H_2S}}\frac{C_{ClOH}}{C^*_{H_2S}}(1-x) + \frac{D_{ClO^-}}{D_{H_2S}}\frac{C_{ClO^-}}{C^*_{H_2S}}(1-y) \text{ with } x = \frac{C^*_{ClOH}}{C_{ClOH}} \text{ and } y = \frac{C^*_{ClO^-}}{C_{ClO^-}} \qquad \text{Eq. 42}$$

Onda et al. (1970) proposed an approximate solution of the differential equations system obtained by linearization. For two second-order reactions:

$$E = \frac{\sqrt{M_2}\left(1 - \frac{C_{H_2S}}{C^*_{H_2S}}\frac{1}{\cosh\left(\sqrt{M_2}\right)}\right)}{\left(1 - C_{H_2S}/C^*_{H_2S}\right)\tanh\left(\sqrt{M_2}\right)} \approx \frac{\sqrt{M_2}}{\tanh\left(\sqrt{M_2}\right)} \qquad \text{Eq. 43}$$

With:

$$M_2 = \frac{k_7 D_{H_2S} C_{ClOH}}{k_L^{\,2}}\left(x + \frac{k_6}{k_7}\frac{C_{ClO^-}}{C_{ClOH}}y\right) \qquad \text{Eq. 44}$$

Eqs. 42 and 43 are two independent equations with 3 variables (*x*, *y* and *E*). Therefore, an additional equation is required. Onda et al. (1970) assumed that the reagent concentrations are quadratic functions of the film thickness and obtained the following equation:

$$y = \frac{1 - \frac{1}{6}\frac{D_{ClOH}}{D_{ClO^-}}\frac{k_6}{k_7}(1-x)}{1 + \frac{5}{6}\frac{D_{ClOH}}{D_{ClO^-}}\frac{k_6}{k_7}\frac{1-x}{x}} \qquad \text{Eq. 45}$$

Following the numerical procedure developed in the supplementary material, k_6 ($6.75\ 10^6$ L mol^{-1} s^{-1}) and k_7 ($1.62\ 10^5$ L mol^{-1} s^{-1}) were determined by the least square method trying to minimize the error between the experimental and theoretical values of *E* (procedure presented in the supplementary material). These values confirm the order of magnitude expected by Biard et al. (Biard et al., 2010). The determined apparent kinetic constant of H_2S with ClO^- is larger than the one with ClOH which

corroborates the assumption that H_2S can react with ClO^- through an acid base reaction before oxidation. To assess the importance of both reactions with ClO^- and ClOH, the ratio (E_{39}/E_{39+40}) of the enhancement factor calculated assuming just the reaction with ClO^- on the overall enhancement factor has been calculated (Table 4). It confirms that, except for circumneutral and basic pH, both reactions contribute to the overall mass transfer enhancement.

The relative errors between the experimental and theoretical values of Eff_{H_2S} are summarized in Table 4 and confirm a rather good agreement of the model. In the one hand, the discrepancy between the experimental and theoretical values of *E* is rather large (average error of 24%) since the determination of *E* is very sensitive to the experimental uncertainties (on *Eff*, Q_G and the *pH* especially). In other words, even low experimental uncertainties induce a rather large uncertainty on *E*. However, the points are distributed on both sides of the parity plot excluding systematic errors (Fig. 5). On the other hand, calculations of theoretical values of Eff_{H_2S} are poorly sensitive to *E*. By the way, the difference between the experimental and theoretical values of Eff_{H_2S} is really low (3.8% in average). These observations are emphasized by the sensitivity analysis (§ 4.5.3).

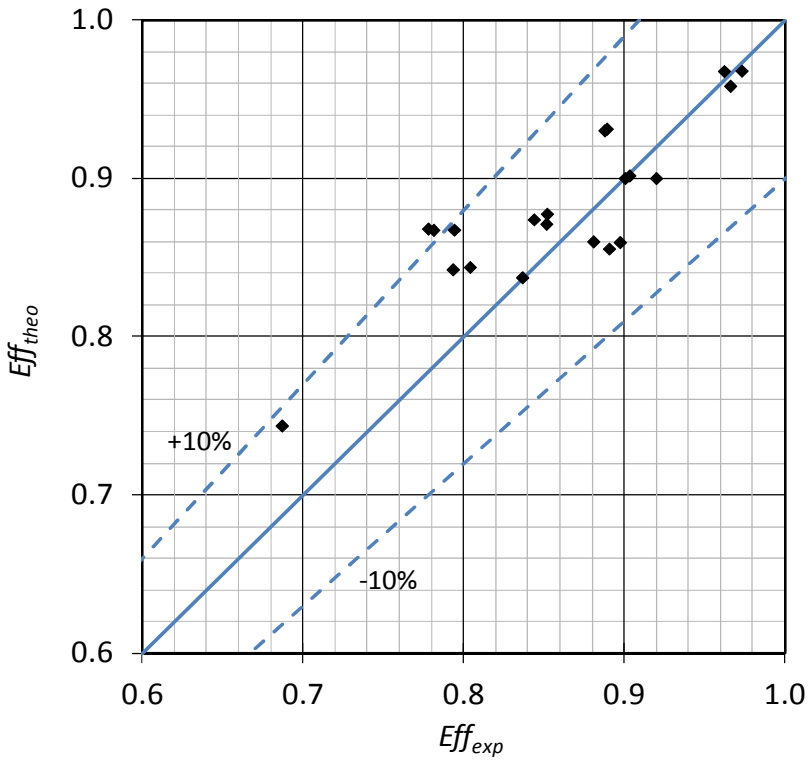

Figure 5: Parity plot between the experimental and predicted removal efficiencies during H_2S absorption in chlorine solutions.

At basic pH, reaction 34 should not be neglected anymore. A competition between Eq. 34 and 36 is expected depending on the pH and the total chlorine concentration. In the next step of this project, k_6 and k_7 will be confronted to the kinetic constants that we measured for HS^- oxidation by chlorine

(result not published yet) to build a kinetic model at basic pH. More complex numerical resolution tools will be required to solve the high numbers of differential equations and finally build a model which can provide an efficient tool for scrubbers design.

4.5.3 Sensitivity analysis

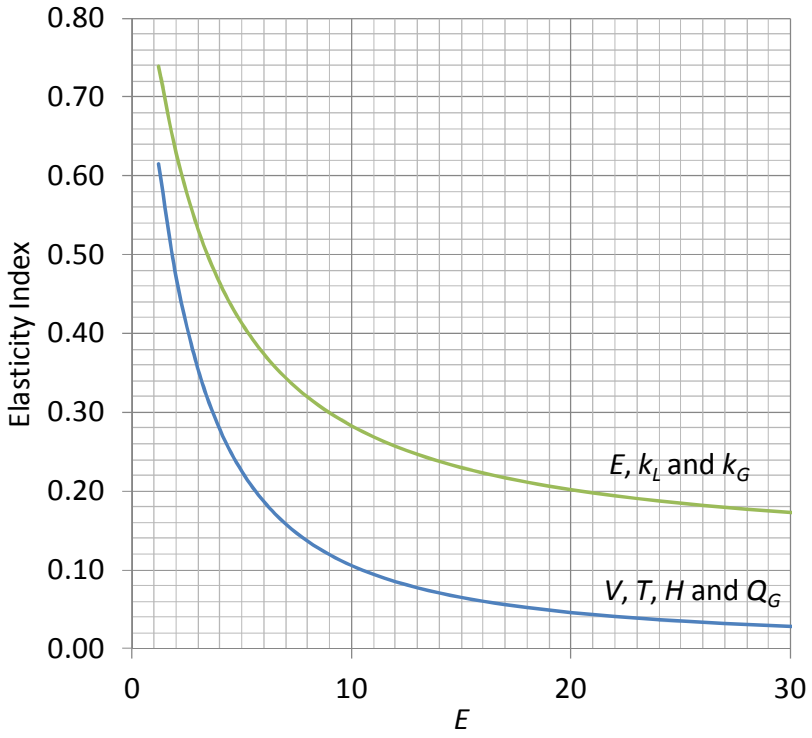

Figure 6: The Eff_{H_2S} Elasticity Index vs. the enhancement factor for several inputs.

The sensitivity analysis quantifies the influence of the input E, k_L, k_G, V and T on the output Eff_{H_2S} (Fig. 6) for increasing values of E. The three most significant inputs are E, k_L and k_G which directly influence the mass transfer rate. Errors on the enhancement factor determination (due to uncertainties on k_6 and k_7) are more significant for low values of E with more liquid phase resistance. With significant chlorine concentrations up to 500 ppm at alkaline pH, the kinetics of oxidation is so large that the resistance in the liquid phase is almost negligible and the mass transfer rate is controlled by the gas phase. This conclusion obtained with a well agitated reactor can be extrapolated to packed column widely used in gas treatment. Therefore, designers must adjust their concentration to insure an excess of chlorine in order to maintain a low liquid phase resistance in the whole gas-liquid contactor, especially at the bottom where chlorine has been partly consumed.

5 Conclusions

Kinetics of H_2S reaction with hypochlorite anion and hypochlorous acid was investigated by reactive absorption in a well agitated gas-liquid contactor. The liquid and gas sides mass transfer coefficients as well as the interfacial area has been determined using appropriated experimental conditions. These values were confirmed with the modeling of reactive absorption of H_2S in water without oxidant. Absorption of H_2S in chlorine solutions demonstrated that the oxidation kinetic rate increases surprisingly with the pH which highlights that HS^- may play a role in the oxidation mechanism. We assumed that H_2S reacts with ClO^- to form HS^- which is further oxidized by ClOH to build a global mechanism based on the H_2S irreversible reactions with ClO^- (k_6 = 6.75 10^6 L mol^{-1} s^{-1}) and ClOH (k_7 = 1.62 10^5 L mol^{-1} s^{-1}). A good agreement between the experimental and the theoretical values of the removal efficiencies confirmed the order of magnitude of the kinetic constants found and the validity of the model at the pH range tested. The next step of this study will require to improve the model for the description of the mechanism at basic pH.

6 Acknowledgements

The authors wish to thank Candelà De La Sota Sandez for her participation to the RTD measurements and Dominique Allaire for his contribution to the set-up construction. We also wish to thanks Christophe Renner from Veolia Environnement Recherche et Innovation (Maisons-Laffitte) for his material contribution to this project.

References

Aieta, E.M., Roberts, P.V., 1986. Application of mass transfer theory to the kinetics of a fast gas-liquid reaction: chlorine hydrolysis. Environ. Sci. Technol. 20, 44-50.

Asadi Kalameh, H., Karamali, A., Anitescu, C., Rabczuk, T., 2012. High velocity impact of metal sphere on thin metallic plate using smooth particle hydrodynamics (SPH) method. Front. Struct. Civ. Eng. 6, 101-110.

Beltrán, F.J., 2004. Ozone reaction kinetics for water and wastewater systems. CRC Press, Boca Raton.

Biard, P.-F., 2009. Contribution au développement d'un procédé de lavage chimique compact. Traitement du sulfure d'hydrogène par le chlore à l'échelle semi-industrielle et de COV odorants par oxydation avancée O_3/H_2O_2 à l'échelle du laboratoire., ENSCR. University of Rennes 1, Rennes, p. 229.

Biard, P.-F., Couvert, A., 2013. Overview of mass transfer enhancement factor determination for acidic and basic compounds absorption in water. Chem. Eng. J. 222, 444-453.

Biard, P.-F., Couvert, A., Renner, C., Levasseur, J.-P., 2010. Wet scrubbing intensification applied to hydrogen sulphide removal in waste water treatment plant. Can. J. Chem. Eng. 88, 682-687.

Biard, P.-F., Couvert, A., Renner, C., Zozor, P., Bassivière, S., Levasseur, J.-P., 2009. Hydrogen sulphide removal in waste water treatment plant by compact oxidative scrubbing in Aquilair Plus™ process. Wat. Practice. technol. 4, doi:10.2166/wpt.2009.2023.

Bonnin, C., 1991. Les sources de nuisances olfactives dans les stations de traitement des eaux usées résiduaires, et leur traitement par lavage à l'eau chlorée en milieu basique, Ecole Nationale Supérieure de Chimie de Rennes. Université de Rennes I, Rennes, p. 191.

Brettschneider, O., Thiele, R., Faber, R., Thielert, H., Wozny, G., 2004. Experimental investigation and simulation of the chemical absorption in a packed column for the system NH_3–CO_2–H_2S–NaOH–H_2O. Sep. Purif. Technol. 39, 139-159.

Busca, G., Chiara, P., 2003. Technologies for the abatement of sulphide compounds from gaseous streams: a comparative overview. J. Loss. Prev. Process Indust. 16, 363-371.

Calderbank, P., 1958. Physical rate processes in industrial fermentation - Part I: The interfacial area in gas-liquid contacting with mechanical agitation. Chem. Eng. Res. Des. 36, 443-463.

Calderbank, P.H., 1959. Physical rate processes in industrial fermentation - Part II: Mass transfer coefficients in gas-liquid contacting with and without mechanical agitation. Chem. Eng. Res. Des. 37, 173-185.

Chang, C.S., Rochelle, G.T., 1982. Mass transfer enhanced by equilibrium reactions. Ind. Eng. Chem. Fund. 21, 379-385.

Chao, M., 1968. The diffusion coefficients of hypochlorite, hypochlorous acid, and chlorine in aqueous media by chronopotentiometry. J. Electrochem. Soc. 115, 1172.

Chen, L., Huang, J., Yang, C.-L., 2001. Absorption of H_2S in NaOCl caustic aqueous solution. Environ. Prog. 20, 175-181.

Choppin, A.R., Faulkenberry, L.C., 1937. The oxidation of aqueous sulfide solutions by hypochlorites. Journal of the American Chemical Society 59, 2203-2207.

Deborde, M., Von Gunten, U., 2008. Reactions of chlorine with inorganic and organic compounds during water treatment - Kinetics and mechanisms: A critical review. Wat. Res. 42, 13-51.

Ebrahimi, S., Picioreanu, C., Kleerebezem, R., Heijnen, J.J., van Loosdrecht, M.C.M., 2003. Rate-based modelling of SO_2 absorption into aqueous $NaHCO_3/Na_2CO_3$ solutions accompanied by the desorption of CO_2. Chem. Eng. Sci. 58, 3589-3600.

Eigen, M., 1964. Proton transfer, acid-base catalysis, and enzymatic hydrolysis. Part I: elementary processes. Angewandte Chem. Int. Edition in English 3, 1-19.

Fernández-Prini, R., Alvarez, J.L., Harvey, A.H., 2003. Henry's constants and vapor-liquid distribution constants for gaseous solutes in H_2O and D_2O at high temperatures. J. Phys. Chem. Ref. Data 32, 903-916.

Foussard, J.-N., Debellefontaine, H., 2000. Thermodynamic basis for the solubility and diffusivity of ozone in water, IOA International specialised symposium, fundamental and engineering concepts for ozone reactor design, Toulouse, pp. 35-38.

Gostelow, P., Parsons, S.A., Stuetz, R.M., 2001. Odour measurements for sewage treatment works. Wat. Res. 35, 579-597.

Hikita, H., Asai, S., 1964. Gas absorption with (m, n)th order irreversible chemical reaction. Int. Chem. Eng. 4, 332–340.

Hoffmann, A., Mackowiak, J., Gorak, A., Haas, M., Loning, J., Runowski, T., Hallenberger, K., 2007. Standardization of mass transfer measurements: a basis for the description of absorption processes. Chem. Eng. Res. Des. 85, 40.

Jia, Y., Zhong, Q., Fan, X., Wang, X., 2010. Kinetics of oxidation of total sulfite in the ammonia-based wet flue gas desulfurization process. Chem. Eng. J. 164, 132-138.

Jing, G., Zhou, L., Zhou, Z., 2012. Characterization and kinetics of carbon dioxide absorption into aqueous tetramethylammonium glycinate solution. Chem. Eng. J. 181–182, 85-92.

Joshi, J., Pandit, A., Sharma, M., 1982. Mechanically agitated gas-liquid reactors. Chem. Eng. Sci. 37, 813-844.

Kangas, J., Jäppinen, P., Savolainen, H., 1984. Exposure to hydrogen sulfide, mercaptans and sulfur dioxide in pulp industry. AIHA J. 45, 787-790.

Kerc, A., Olmez, S.S., 2010. Ozonation of odorous air in wastewater treatment plants. Ozone Sci. Eng. 32, 199 - 203.

Kohl, A.L., Nielsen, R., 1997. Gas purification. Gulf Professional Publishing.

Kucka, L., Kenig, E.Y., Górak, A., 2002. Kinetics of the gas-liquid reaction between carbon dioxide and hydroxide ions. Ind. Eng. Chem. Res. 41, 5952-5957.

Langlais, B., Reckhow, D.A., Brink, D.R., 1991. Ozone in water treatment. Chelsea, MI (United States) ; Lewis Publishers, United States.

Lara Marquez, A., Wild, G., Midoux, N., 1994. A review of recent chemical techniques for the determination of the volumetric mass transfer coefficient k_La in gas-liquid reactor. Chem. Eng. Proc. 33, 247-260.

Le Sauze, N., Laplanche, A., Martin, G., Paillard, H., 1991. A process of washing and ozonation to deodorize an atmosphere contaminated by sulfides. Ozone Sci. Eng. 13, 331-347.

Lee, S.Y., Pang Tsui, Y., 1999. Succeed at gas/liquid contacting. Chem. Eng. Prog. 95, 23-49.

Morris, J.C., 1967. Kinetics of reactions between aqueous chlorine and nitrogen compounds. John Wiley & Sons, New York, NY.

Onda, K., Sada, E., Kobayashi, T., Fujine, M., 1970. Gas absorption accompanied by complex chemical reactions—III Parallel chemical reactions. Chem. Eng. Sci. 25, 1023-1031.

Perry, R.H., Green, D.W., 1997. Perry's chemical engineers' handbook, 7th edition. McGraw-Hill, New-York.

Rappert, S., Müller, R., 2005. Odor compounds in waste gas emissions from agricultural operations and food industries. Waste Manag. 25, 887-907.

Rejl, J., Linek, V., Moucha, T., Valenz, L., 2009. Methods standardization in the measurement of mass transfer characteristics in packed absorption columns. Chem. Eng. Res. Des. 87, 695-704.

RESI, 2013. Gas-liquid mass transfer in gassed mechanically agitated vessels. http://www.resi.com.tw/Mixing/08DOC.pdf.

Roustan, M., 2003. Transferts gaz-liquide dans les procédés de traitement des eaux et des effluents gazeux. Lavoisier, Paris.

Sema, T., Naami, A., Fu, K., Edali, M., Liu, H., Shi, H., Liang, Z., Idem, R., Tontiwachwuthikul, P., 2012. Comprehensive mass transfer and reaction kinetics studies of CO_2 absorption into aqueous solutions of blended MDEA–MEA. Chem. Eng. J. 209, 501-512.

Smet, E., Langenhove, H.V., 1998. Abatement of volatile organic sulfur compounds in odorous emissions from the bio-industry. Biodegradation 9, 273-284.

Smet, E., Lens, P., Langenhove, H.V., 1998. Treatment of waste gases contaminated with odorous sulfur compounds. Crit. Rev. Environ. Sci. Tech. 28, 89-117.

Sotelo, J.L., Beltrán, F.J., Gonzalez, M., Garcia-Araya, J.F., 1991. Ozonation of aqueous solutions of resorcinol and phloroglucinol. 2. Kinetic study. Ind. Eng. Chem. Res. 30, 222-227.

Staehelin, J., Hoigne, J., 1982. Decomposition of ozone in water: rate of initiation by hydroxide ions and hydrogen peroxide. Environ. Sci. Technol. 16, 676-681.

Tamimi, A., Rinker, E.B., Sandall, O.C., 1994. Diffusion coefficients for hydrogen sulfide, carbon dioxide, and nitrous oxide in water over the temperature range 293-368 K. J. Chem. Eng. Data 39, 330-332.

Vaidya, P.D., Kenig, E.Y., 2007a. Absorption of CO_2 into aqueous blends of alkanolamines prepared from renewable resources. Chem. Eng. Sci. 62, 7344-7350.

Vaidya, P.D., Kenig, E.Y., 2007b. Gas–Liquid reaction kinetics: a review of determination methods. Chem. Eng. Comm. 194, 1543-1565.

Vaidya, P.D., Kenig, E.Y., 2009. A Study on CO_2 absorption kinetics by aqueous solutions of N, N-Diethylethanolamine and N-Ethylethanolamine. Chem. Eng. Technol. 32, 556-563.

van Swaaij, W.P.M., Versteeg, G.F., 1992. Mass transfer accompanied with complex reversible chemical reactions in gas—liquid systems: an overview. Chem. Eng. Sci. 47, 3181-3195.

Wang, T.X., Margerum, D.W., 1994. Kinetics of reversible chlorine hydrolysis: Temperature dependence and general-acid/base-assisted mechanisms. Inorg. Chem. 33, 1050-1055.

Whitman, W.G., 1923. A preliminary experimental confirmation of the two-film theory of gas absorption. Chem. Met. Eng. 29, 146-148.

Yin, H., Wu, S., Ejeta, M., 2005. CalSim-II Model Sensitivity Analysis Study: Technical Memorandum Report. california Department of Water Resources, Bay-Delta Office.

Appendix A: Additional tables

Table A. 1 : Compilation of the physico-chemical properties used.

Parameter	Values at 293 K	References
	Water	
ρ_L (kg m^{-3})	1000	
M_L (kg mol^{-1})	0.018	
pK_w	14.15	
	H_2S	
H_{H_2S} (Pa m^3 mol^{-1})	864	(Fernández-Prini et al., 2003)
D_{H_2S} (m^2 s^{-1})	1.75×10^{-9}	(Tamimi et al., 1994)
$pK_{A,2}$ (H_2S/HS^-)	$-\log\left(0.00361\exp\left(-\frac{3131}{T}\right)\right)$ => 7.07 at 293 K	(Roustan, 2003)
$pK_{A,3}$ (HS^-/S^{2-})	$-\log\left(\exp\left(-7.489-\frac{7211.2}{T}\right)\right)$ => 13.94 at 293 K	(Brettschneider et al., 2004)
	O_3	
H_{O_3} (Pa m^3 mol^{-1})	$\exp\left(22.3-\frac{4030}{T}\right)\times1.013\times10^5\times\frac{M_L}{\rho_L}=9400$ Pa.m^3.mol^{-1}	(Langlais et al., 1991)
D_{O_3} (m^2 s^{-1})	1.7×10^{-9}	(Foussard and Debellefontaine, 2000)
k_{O_3/HO_2^-} (m^3 mol^{-1} s^{-1})	$2.8\times10^9 \pm 0.5\times10^9$	(Staehelin and Hoigne, 1982)
	O_2	
H_{O_2} (Pa m^3 mol^{-1})	7.3×10^4	(Roustan, 2003)
D_{O_2} (m^2 s^{-1})	2.1×10^{-9}	(Roustan, 2003)
	$ClOH/ClO^-$	
K_1 (Cl_2 → HClO)	$\left(\exp\left(\frac{53}{R}\right)\exp\left(-\frac{33000}{RT}\right)\right)+1.02\left(\left(\frac{I^{0.5}}{1+I^{0.5}}-\frac{0.5^{0.5}}{1+0.5^{0.5}}\right)+0.23(0.5-I)\right)$ => 3.8×10^{-4} at I = 0 et 293 K	Eq. deduced from (Wang and Margerum, 1994)
$pK_{A,1}$ ($ClOH/ClO^-$)=	$\frac{3000}{T}-10.0686+0.0253\times T$ => 7.58 at 293K	(Morris, 1967)
D_{ClO^-} (m^2 s^{-1})	$10^{\frac{-1060}{T}-5.40}$ => 0.96×10^{-9} at 293K	(Chao, 1968)
D_{ClOH} (m^2 s^{-1})	$10^{\frac{-945}{T}-5.72}$ => 1.13×10^{-9} at 293K	(Chao, 1968)
	H_2O_2/HO_2^-	
$pK_{A,4}$	11.8	(Beltrán, 2004)

Table A.2: Suppliers and references of the chemical products and equipments used.

Chemical products			
NaOH	10 mol L^{-1}	Labogros	France
H_3PO_4	85% wt	Acros Organics	Belgium
NaOCl	13% wt	Acros Organics	Belgium
H_2O_2	35% wt	Acros Organics	Belgium
Acetic acid	99.9%	Acros Organics	Belgium
Indigo carmine	Analytical grade	Acros Organics	Belgium
Sodium thiosulfate	Titrisol® 0.1 mol L^{-1}	Merck	Germany
Potassium iodide	Analytical grade	Acros Organics	Belgium
Ammonium molybdate	98.5 0025	Rectapur VWR	Belgium
O_2 (cylinder)	Pure	Air Liquide	France
N_2/H_2S mixture (cylinder)	1000 ± 50 ppmv in H_2S	Air liquide	France
Equipments			
Float type flowmeters	Brooks Instrument	Sho Rate R6-15-B (liquids) Sho Rate R6-15-C (air) Sho Rate R6-15-D (H_2S/N_2)	USA
Float type flowmeter in Teflon®	Gilmont	GF-1360	USA
Centrifugal pumps	Iwaki	Magnet Pump MD-30FX	Japan
Gas membrane pump	KNF	N816.1.2KN.45.18	France
Static mixer	Koflo	3/8 OD	Japan
Bourdon manometers	Bamo	63 P60.5	France
Ozone generator	Trailigaz	24 g h^{-1} fed with O_2	France
Ion chromatograph	Dionex	DX 120	USA
Ozone analyzer	Trailigaz	Uvozon 200	France
Combined pH-T probe	Schott	Blue Line 14 pH	Germany
O_2 probe	WTW	CellOx 325	Germany

Table A. 3: Results of the ozone absorption experiments using the operating conditions of Table 1.

$C_{H_2O_2,i}$ (mg L^{-1})	$C_{H_2O_2,o}$ (mg L^{-1})	pH	Q_L (L h^{-1})	Q_G (NL h^{-1})	U_{SG} (m s^{-1})	Eff_{O_3} (%)	a° (m^2 m^{-3})	Ha
1173	606	9.9	6.9	482	1.13	21.3	75.1	4.16
1173	538	9.9	6.9	606	1.27	20.8	80.2	3.92
1173	797	9.9	14.0	680	1.34	23.6	76.7	4.78
1173	762	9.9	12.2	762	1.44	21.5	77.7	4.67
1471	1071	10.04	14.0	642	1.18	33.2	76.1	5.93
1471	1197	9.99	21.2	720	1.27	33.6	81.3	6.11
1683	835	10.07	6.9	462	1.18	32.2	77.9	6.93
1683	888	10.07	6.9	496	1.25	28.5	70.0	6.73
1683	1250	10.03	14.0	567	1.36	30.8	71.4	6.91
1683	1262	10	14.0	633	1.44	29.1	72.8	7.56
1794	947	10.15	6.9	500	1.24	33.7	74.7	7.52
1794	1360	10.07	14.0	577	1.34	34.2	71.4	7.58
1794	1375	10.06	14.0	650	1.40	32.8	72.7	7.90
1794	1496	10.03	21.2	754	1.46	33.4	78.3	7.93
2720	1701	10.01	6.9	465	1.18	42.2	85.3	8.29
2720	1792	9.99	6.9	498	1.25	37.8	76.8	8.09
2720	2298	9.92	14.0	594	1.30	34.0	64.8	8.52
2720	2238	9.91	14.0	628	1.45	37.5	85.0	6.49
2720	2425	9.92	21.2	717	1.54	35.1	78.0	6.48